

Velocity fields of distant galaxies with FORS2 at the VLT

Bodo L. Ziegler¹,
Elif Kutdemir²,
Cristiano Da Rocha¹,
Asmus Böhm³,
Wolfgang Kapferer³,
Harald Kuntschner¹,
Reynier F. Peletier²,
Sabine Schindler³,
Miguel Verdugo⁴

¹ESO

²Kapteyn Institute, Groningen, Netherlands

³University Innsbruck, Austria

⁴University Göttingen, Germany

We describe a method to efficiently obtain two-dimensional velocity fields of distant, faint and small, emission-line galaxies with FORS2 at the VLT. They are examined for kinematic substructure to identify possible interaction processes. Numerical simulations of tidal interactions and ram-pressure effects reveal distinct signatures observable with our method. We detect a significant fraction of galaxies with irregular velocity fields both in the field and cluster environments.

Galaxy formation and evolution are still principal research topics in modern astrophysics although having been investigated since the recognition of objects outside the Milky Way after the Great Debate between Shapley and Curtis. The main questions include: When and how did galaxies form? Why are there different morphological types? What is the role of environment? Models range from single epoch to continuous creation scenarios. The current theoretical paradigm of a cold dark matter dominated universe predicts a hierarchical bottom-up structure evolution from small entities towards bigger systems through merging. During such a process spiral galaxies can be transformed into ellipticals, however, the disc component can be regained through subsequent new gas accretion and star formation. Many irregular and peculiar galaxies are observed in clusters of galaxies, in which they may experience interactions in addition to merging and accretion.

Much progress was achieved in recent years by deep photometric surveys (like GOODS) finding galaxies and quasars at high redshift ($z \sim 6$) corresponding to an epoch just a billion years after the Big Bang and revealing a dichotomy between blue star forming and red passive galaxies at later times with an evolutionary transition between the two groups. Spectroscopic surveys (like CFHRS) additionally produced evidence that there is a sharp decline in the overall star formation activity in the cosmos within the last eight billion years. However, all these results are based on measurements of the luminosity as produced by the stars, while the total mass of a galaxy is mainly composed of dark matter. Because the triggering and process of star formation contains complicated physics, we need to make many assumptions and simplifications in our modeling, and, in addition, we do not clearly understand the scaling between the baryonic and dark matter. Therefore, it would be more favourable if we could observationally determine the total mass of galaxies and compare its evolution directly to the predicted structure assembly.

Such measurements of the dynamical mass even of faint and small, very distant galaxies were achieved recently by a number of research groups using the largest telescopes. Through spectroscopy they derive the internal kinematics (motions) of the stellar system that are subject to the whole gravitational potential. In the optical wavelengths regime, we can conduct this out to redshifts of unity. For spiral galaxies, we can determine the rotation curve from gas emission lines (like [O II] at 372.7nm restframe wavelength). If the galaxy is undisturbed, the rotation curve rises in the inner part and turns over into a flat plateau dominated by its dark halo and we can calculate the maximum rotation velocity V_{\max} . In such a case the assumption of virialization holds, so that we can use the Tully-Fisher relation TFR (Tully & Fisher 1977) as a powerful diagnostic tool that scales the baryonic matter (parameterised, e.g., by stellar luminosity) to the dark matter (as given by V_{\max}). Our group, for example, has found that the TFR of 130 distant ($z=0.5$ on

average) field galaxies has a shallower slope than the local one if restframe B-band luminosities are considered, so that the brightening of a slowly rotating spiral is much larger than the one of a fastly rotating galaxy (Böhm & Ziegler 2007). This result can be interpreted principally in two ways: either the majority of distant galaxies are much more scattered around the TFR and we do not see enough regular spirals at the faint end or there is a mass-dependent evolution with low-mass objects exhibiting on average a stronger effect over the last five billion years. The latter scenario is supported by chemical evolution modeling of our galaxies that revealed less efficient but extended star formation for slow rotators (Ferreras et al. 2004) and is consistent with other observational evidence for a mass-dependent evolution (often called “downsizing”).

For a correct application of the TF analysis it is indispensable that a galaxy is undisturbed so that the assumption of virial equilibrium is fulfilled and, therefore, the rotation curve shows a very regular shape. If this is not the case, can we then still learn something? In the CDM structure formation theory, galaxies evolve by merging and accretion, so that we can look for kinematic signatures of such events and whether there is an increase in the abundance of such types with redshift. To investigate a possible environmental dependence, we need to disentangle such collisions from numerous other interaction phenomena galaxies can experience in groups and clusters. The gas content of spirals reacts to the ram-pressure exerted by the intracluster medium, a hot plasma permeating the whole structure. Part of the gas can also be stripped off by tidal forces (sometimes called “strangulation”). Other processes like harassment can even remove stars from galaxy discs, so that the overall morphology gets altered. However, (irregular) rotation curves from slit spectroscopy do not contain unique information to reveal unambiguously a specific interaction process. In addition, peculiar shapes can sometimes be caused artificially by observational and instrumental effects when long-slits are used (Ziegler et al. 2003, Jäger et al. 2004). A more favourable observation would, therefore, be that of a two-dimensional velocity field.

FORS2 spectroscopy to obtain velocity fields

Many large telescopes today offer 3D-spectroscopy and most future facilities (like E-ELT) will provide such instrument modes. At the VLT, for example, VIMOS and FLAMES offer IFU spectroscopy in the optical regime. For our specific purpose, however, we conceived a different method to obtain velocity fields that has many advantages for our science case: matched galaxy sizes, good spatial resolution, long wavelength range and high efficiency through a large number of simultaneous targets and economic exposure times (Ziegler et al. 2007, Kutdemir et al. 2008).

For our procedure, we utilise the MXU mode of FORS2 that allows to cut slits individually and at any desired orientation into a mask by a laser. We pick up a particular target and start with a slit placing it along the photometric major axis as measured on spatially highly resolved HST/ACS images (Figure 1). The slit covers the full size of the galaxy in its mid-plane with width 1” and extends much beyond it to allow an accurate sky subtraction (common slit lengths are 15-25”). In the same manner, 20-30 more slits are placed on other targets across the full field of view of FORS2 (6.8’ x 6.8’); occasionally even two or three objects fall into the same slit. Observations of such a mask will yield in the end rotation curves like for our previous projects with one spatial axis and one velocity axis by measuring centre positions of an emission line row-by-row along the spatial profile of the two-dimensional galaxy spectrum (Böhm et al. 2004). In order to construct a velocity field with two spatial axes we observe all targets twice again with different slit positions using two more masks. This time slits are placed 1” offset along the minor axis of the galaxy to either side of the first position, so that all three slit positions together correspond to a rectangular grid (Figure 1). That way, the full extent of a galaxy is covered, which is particularly important for a TF galaxy, where we need to measure the flat part of the rotation curve, which is usually reached at about three disc scale lengths. At the redshifts of our targets (0.1 - 1.0), this corresponds to angular sizes of about 3” to 6”. The spatial resolution along the x-axis of our grid is given by the pixel size of the FORS2 CCD chips of 0.25”. For the y-axis, we are restricted by the slit width of 1.0”, which is a good compromise between minor losses of light not falling into the slit due to seeing, adequate spectral resolution (R=1000), and spatial sampling in the y-direction.

As spectral element we use a high-throughput holographic VPH grism (600RI) that results in a long wavelength range (330nm) projected onto the CCD with two advantages: for each galaxy several gas emission lines are visible and many absorption lines of the stellar continuum can be combined to derive the stellar rotation curve in addition to the gaseous one. Depending on the redshift of the

object, emission lines from the blue [O II] line (at 372.7nm) to the red H α line (at 656.3nm) are visible. While up to seven different lines can be observed in case of some field galaxies, most cluster members have four (Figure 2). This allows us to derive rotation curves and velocity fields in several independent ways and to check for consistency but also to investigate possible dependencies on the physical state of the gas clouds that emit the respective lines (all galaxies have both recombination and forbidden lines). From line ratios, we can then construct metallicity maps and assess a possible contribution from AGN activity in addition to star formation.

Despite the need for the observation of three masks to construct a velocity field, our method is still highly efficient. The VPH grism with its medium spectral resolution together with the excellent optics of FORS2 makes it possible that with 2.5 hours total integration time, sufficient signal is reached in an emission line to measure accurately line centres in each spectral (CCD) row. This holds also for the outer regions of the galaxies, where the surface brightness drops to low values (from typically 22Vmag/arcsec² in the inner part to about 26Vmag/arcsec²). Therefore, we can obtain the necessary data of a high number of objects (20-30) within a total integration time of only 7.5 hours. For comparison, FLAMES observations with 15 IFUs of similar targets need integration times of 8-13 hours.

The standard reduction of the spectroscopic images produces a wavelength calibrated two-dimensional spectrum for each slit position of the mask separately. Thanks to the high stability of FORS, exposures of the same mask taken in different nights can be combined to a single deep spectrum. Like for the determination of rotation curves, the wavelength of the centre position of a given emission line is measured along the spatial profile. Differences to a common systemic centre can then be translated into velocity space applying Doppler's rule. The construction of the velocity field VF needs a very careful combination of the measurements from the three slit positions. In order to know the exact position of the masks relative to each other, we also included a few stars with narrow slits perpendicular to each other. These stellar spectra are also used to determine the seeing during the exposure. In addition, only for a third of the galaxies per mask the central slit position was taken while the other two thirds had the off-centre positions alleviating both mask acquisition during observations and mask combination after data reduction. To setup the VF, each position-velocity data point is then calculated within a shared coordinate system, whose origin was determined from the intensity maximum of the spatial profile around the emission line in the central slit and its respective wavelength. An example is shown in Figure 3.

Kinematic analysis of velocity fields

Since our VFs cover a large fraction of a galaxy's extent with good spatial resolution, we can analyse them quantitatively to some detail. We use kinemetry (Krajnovic et al. 2006) that was originally developed for nearby galaxies observed with the SAURON 3D-spectrograph, whose VFs have much higher signal and resolve much smaller physical scales than in the case of our distant targets. In polar coordinates the velocity profile of a flat rotating disc can be described by a cosine function of the azimuthal angle. Best fitting ellipses, along which the velocity profiles are extracted, can be determined as a function of radius. Deviations from these fits can be quantified by a harmonic Fourier expansion, whose coefficients can be interpreted in terms of physical parameters. While the first order reflects the bulk motion (the rotation), the third and fifth order, for example, describe the correction to simple rotation and indicate separate kinematic components. For the reconstruction of the intrinsic velocity map free parameters are the flattening and position angle of the ellipses, while their centres are fixed to a common origin. An example of a reconstructed velocity map with best-fitting ellipses overplotted is given in Figure 4. When, instead, the inclination and position angle are fixed to their average global value, a simple rotation field along the kinematic major axis can be modeled. Its residuals with respect to the observed VF may indicate noncircular velocity components like streaming motions along spiral arms or along a bar. Additional components such as a decoupled core can be recognized in such a residual map, too, but also by twists in the position angle and flattening as well as an increase in the k_5 Fourier coefficient. A rotation curve is extracted from the observed VF along the kinematic major axis to accurately determine V_{\max} , which may be different from the one derived from the curve along the central slit aligned with the photometric axis.

Simulations of interactions: structure & kinematics

One of the main goals of our project is to identify signatures of possible interaction events. Galaxies may be transformed from one type into another by merging or accretion but also by other effects like ram-pressure stripping or harassment in the environment of a cluster or group. Open questions are still, which processes are efficient under what conditions and whether there is a dominant mechanism responsible for the abundance of elliptical galaxies in local rich clusters. In order to study systematically the distortions and irregularities in rotation curves and velocity fields caused by interaction phenomena, we perform N-body/SPH simulations and extract both structural and kinematic information from computer output in the same manner as from observational data. The numerical calculations are made for the three components dark matter halo, stellar body and collisional gas clouds of a galaxy and are based on the Gadget2 code (Springel 2005) that incorporates hydrodynamic physics (and has explicit prescriptions for star formation and feedback). So far, we have modeled minor and major mergers, tidal interactions caused by fly-bys, and ram-pressure stripping (Kronberger et al. 2006, 2007, 2008). There are large variations in the degree of distortions both in stellar structure and gas kinematics in case of the first three processes with main dependencies on the mass ratio of the galaxies, the geometry of the interaction in real space and the projection onto the sky plane (the viewing angle of the observations). In the case of a major merger, however, there is always a clear signal in the higher-order coefficients of kinemetry's Fourier decomposition (Figure 5). Ram-pressure by the intracluster medium, on the other hand, mainly affects the gas disc pushing away the outer parts creating distortions at the edge of VFs, while regular rotation can be maintained in the inner regions (Figure 6). In certain configurations, the gas disc can also be displaced from the centre of the stellar disc. During the stripping event, gas can also be compressed so that enhanced star formation is triggered, leading to changes in the stellar populations, too (Kapferer et al. 2009).

In addition, we utilise the simulations in order to systematically investigate how velocity fields and characteristic parameters are influenced by the instrumental and observational setup (like spectral resolution, seeing) and for which cases artificial distortions can be induced (Kapferer et al. 2006). A major impact is caused by the decreasing spatial resolution of the spectra when galaxies are observed at higher and higher redshifts. Minor irregularities can be completely smeared out due to seeing and resolution elements being too coarse.

Currently, we are in the process of analyzing each observed galaxy individually. In case of a regular VF, we perform a TF analysis deriving the rotation curve along the kinematic major axis. For irregular galaxies we examine both the VF and the stellar structure (as revealed on our HST/ACS images) and compare them to a suite of simulated events taking into account the specific galaxy parameters in order to pin down the specific interaction mechanism that caused the distortions.

Velocity fields of distant galaxies

The spectroscopic observations for the presented method were performed in Periods 74 & 75 in four different cluster fields (MS1008.1-1224 $z=0.30$, MS2137.3-2353 $z=0.31$, Cl0412-65 $z=0.51$, MS0451.6-0305 $z=0.54$). The target galaxies were not only cluster members but also field galaxies in the background and foreground ($0.1 < z < 0.9$), so that we can investigate different environments. All cluster fields were imaged with ACS onboard HST enabling an accurate assessment of morphological structure of the galaxies as well. Our method presented here yielded velocity fields for 49 objects with good signal-to-noise appropriate for our kinematic analysis. Out of these, there are 16 VFs suitable for our investigation of possible interaction processes in rich clusters.

In addition to our detailed analysis with comparison to the simulations, we also investigate average properties to assess the abundance of galaxies that have irregular kinematics irrespective of any assumption of a particular interaction process. To that purpose, we quantify deviations from a simple smooth rotation field with three different indicators measured for each galaxy in the same way. As pure gas kinematic tracers we use 1) σ_{PA} : the standard deviation of the kinematic position angles of the best-fitting ellipses found by kinemetry across a galaxy and 2) $k_{3,5}/k_1$: an average value of higher-order Fourier coefficients normalised by the rotation velocity. The third parameter compares the global velocity field determined by spectral lines emitted by the (warm) gas content of a galaxy to its morphological structure seen in the continuum light of the stars: 3) $\Delta\phi$: the mean difference between photometric and kinematic position angles across a galaxy. To find an

appropriate limit of the value range, below which a galaxy can still be classified as undistorted, we measured the three parameters first for a local sample (taken from Daigle et al. 2006) of 18 galaxies that have high-resolution VFs (Kutdemir et al. 2008).

For our distant sample, we find that the fraction of galaxies classified to be irregular according to the three indicators is not unique. For the pure kinematic tracers we derive a much lower percentage (about 10% and 30%) than for the third parameter (about 70%) (Figure 7 and Kutdemir et al. 2009). The parameters trace different signatures of external processes but are also sensitive to intrinsic properties. For example, the presence of a bar misaligned to the disc's major axis can also cause a large offset between the gas field and the stellar component. In addition, peculiarities in a VF are more affected by a coarse spatial binning and could be "smeared out". Modeling resolution effects we found that the irregularity fractions we measure are lower limits only.

Furthermore, our simulations show that only strong interactions like major mergers induce large values of the kinematic tracers indicating big distortions with high significance. So, most of our observed objects with smaller values of the irregularity parameters probably undergo more subtle events. This is presumably also the reason for the surprisingly similar abundance of peculiar galaxies in the field and cluster environment no matter what indicator is chosen. Since we detect more irregular field galaxies at intermediate redshifts than in the local sample, we probably witness the ongoing growth of their discs via accretion and minor mergers as predicted in CDM models. To decisively clarify the ongoing processes both for field and cluster galaxies, we will in the near future examine all available pieces of information for each galaxy (gas VFs, stellar rotation curves, morphologies, stellar populations) and compare them to our simulations.

Acknowledgements: This work was financially supported by VolkswagenStiftung (I/76 520), DFG (ZI 663/6), DLR (50OR0602, 50OR0404, 50OR0301) and Kapteyn institute. Based on observations ESO PID 74.B-0592 & 75.B-0187 as well as HST PID 10635.

Böhm et al. 2004 A&A 420, 97
Böhm & Ziegler 2007 ApJ 668, 846
Ferreras et al. 2004 MNRAS 355, 64
Daigle et al. 2006 MNRAS 367, 469
Jäger et al. 2004 A&A 422, 941
Kapferer et al. 2006 A&A 446, 847
Kapferer et al. 2009 A&A 499, 87
Krajinović et al. 2006 MNRAS 366, 787
Kronberger et al. 2006 A&A 458, 69
Kronberger et al. 2007 A&A 473, 761
Kronberger et al. 2008 A&A 483, 783
Kutdemir et al. 2008 A&A 488, 117
Kutdemir et al. 2009 A&A in prep.
Springel 2005 MNRAS 364, 1105
Tully & Fisher 1977 A&A 54, 661
Ziegler et al. 2003 ApJL 598, 87
Ziegler et al. 2007 IAU Symp. 235, 258

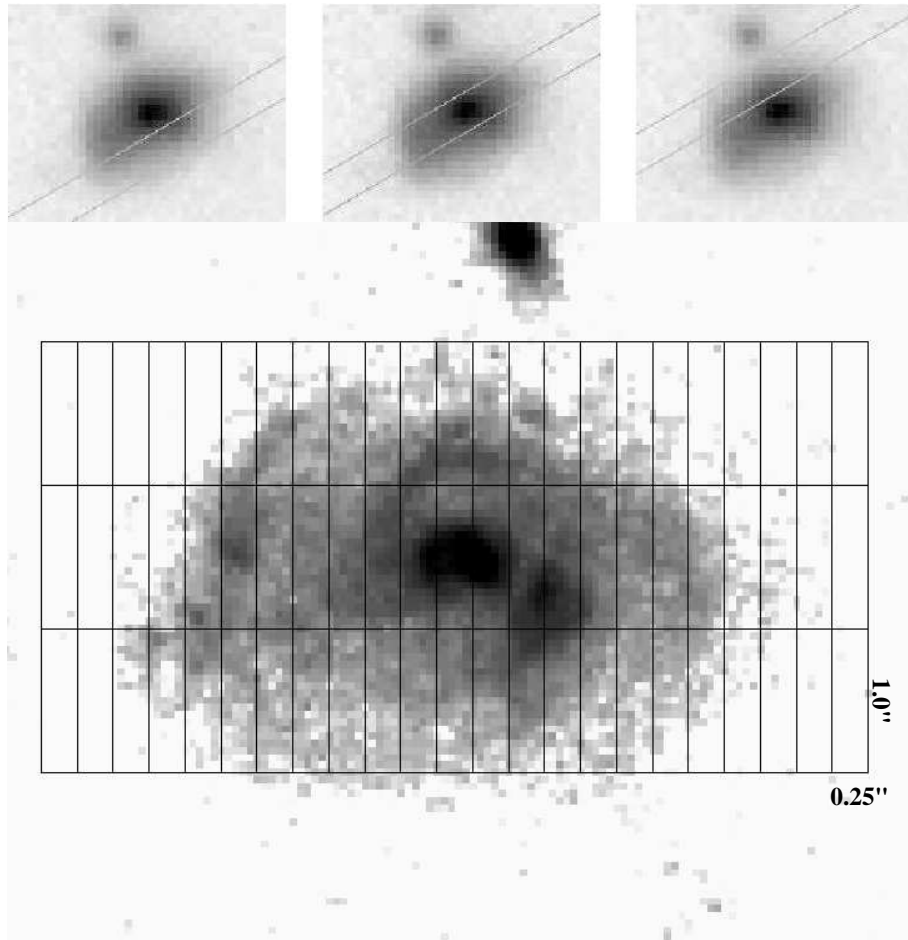


Figure 1: Our method to obtain two dimensional velocity fields with FORS2 is based on the observation of three different slit positions per target. The combination of the measurements yield independent data points for a rectangular grid covering the whole galaxy (from Kutdemir et al. 2008).

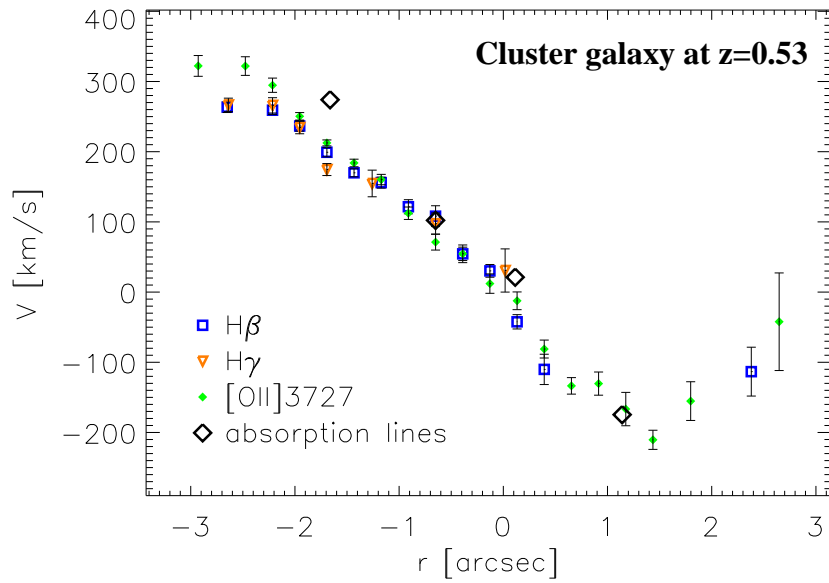
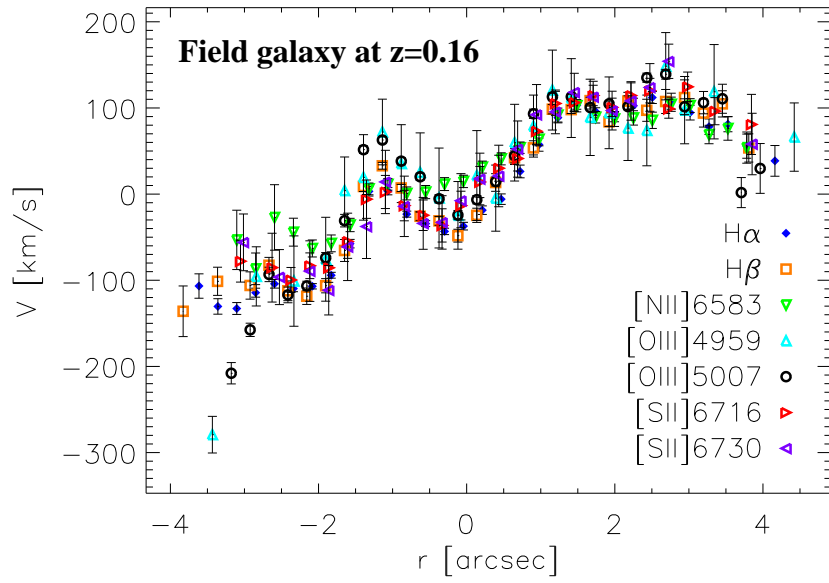


Figure 2: Two examples of rotation curves derived from the central slit. For some field galaxies up to seven different emission lines can be used independently to study the gas kinematics. For brighter galaxies, even stellar rotation curves can be measured by combining many absorption lines (from Kutdemir et al. 2008).

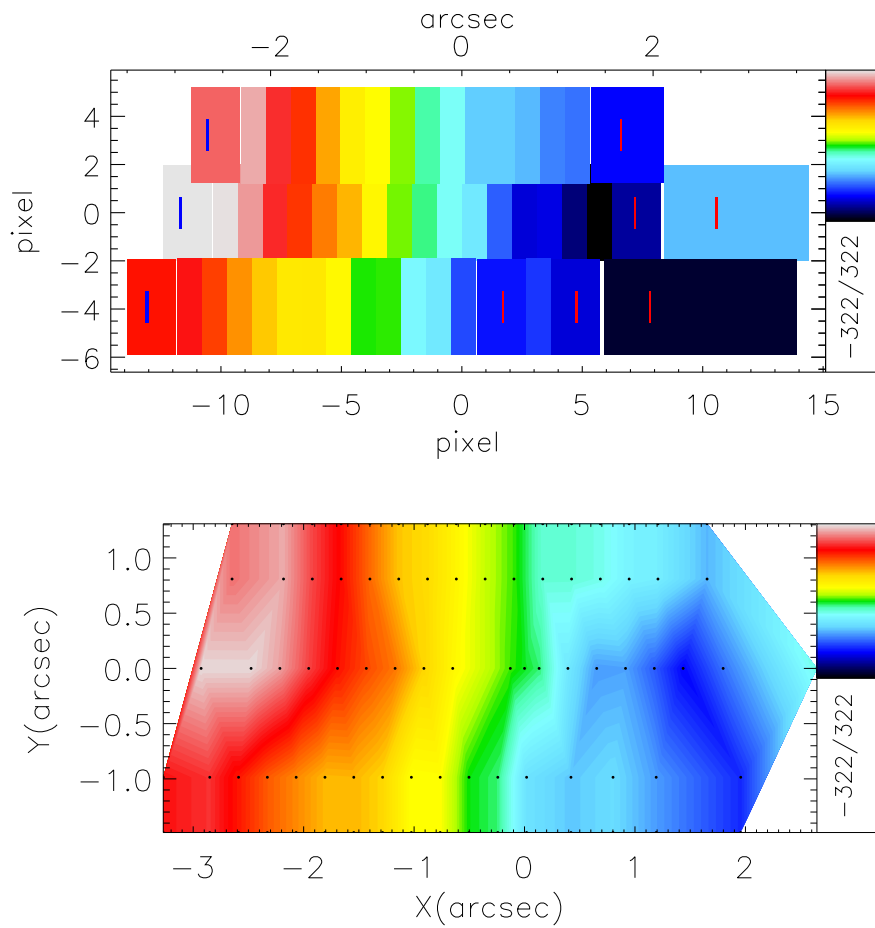


Figure 3: Example of an observed velocity field of a cluster spiral at $z=0.5$ displayed as binned independent data points (top panel) and linearly interpolated for visualisation purposes (bottom panel) (from Kutdemir et al. 2008).

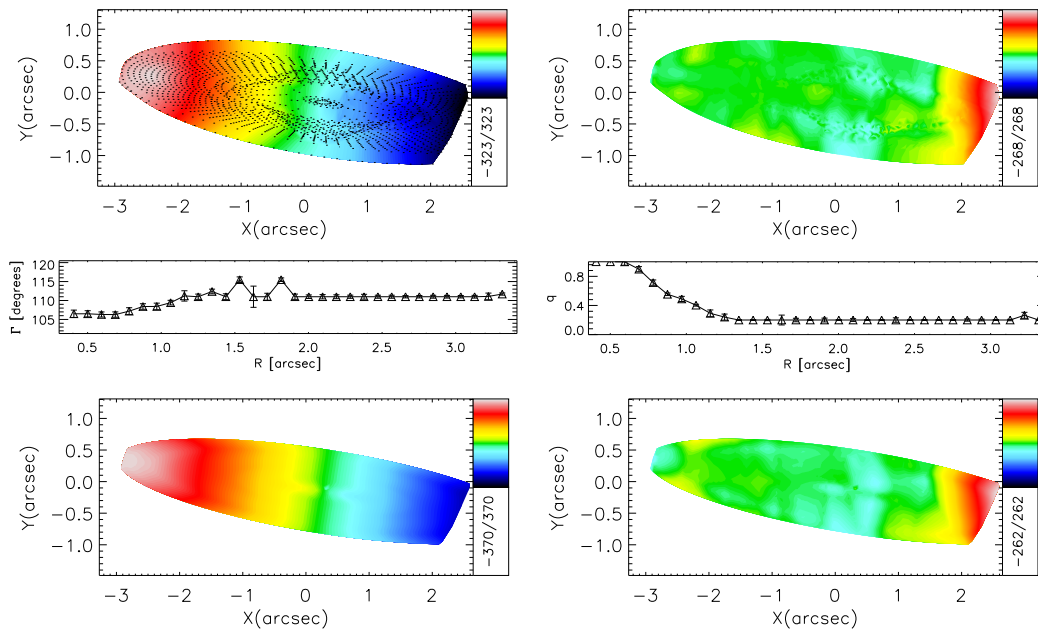


Figure 4: Velocity field of galaxy of Figure 3 reconstructed by kinemetry with best-fitting ellipses overplotted (top left) and its residual map (top right) obtained by subtracting the model from the observed field. Displayed in bottom panels is the model (left) and its residual (right) of the circular velocity component (rotation map) constructed for the average value of the kinematic position angle Γ and flattening q . Radial profiles of the latter parameters are shown in middle panels as function of distance to kinematic centre (from Kutdemir et al. 2008).

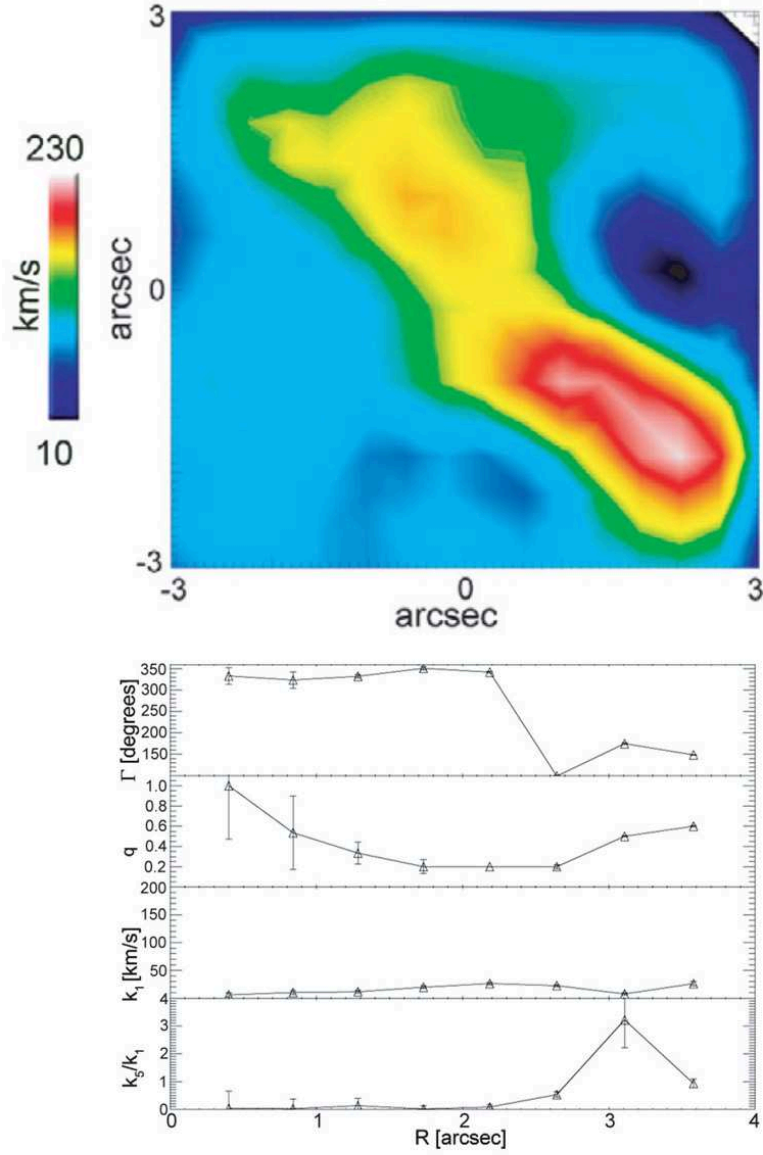


Figure 5: Velocity field of a simulated major merger with spatial resolution corresponding to observations at $z=0.1$ and radial profiles of some parameters determined by kinemetry (kinematic position angle, flattening, first Fourier coefficient indicating the bulk motion and normalised fifth Fourier coefficient indicating separate kinematic components). The case shown refers to a small galaxy that has penetrated a bigger one, 200Myr after the event (from Kronberger et al. 2007).

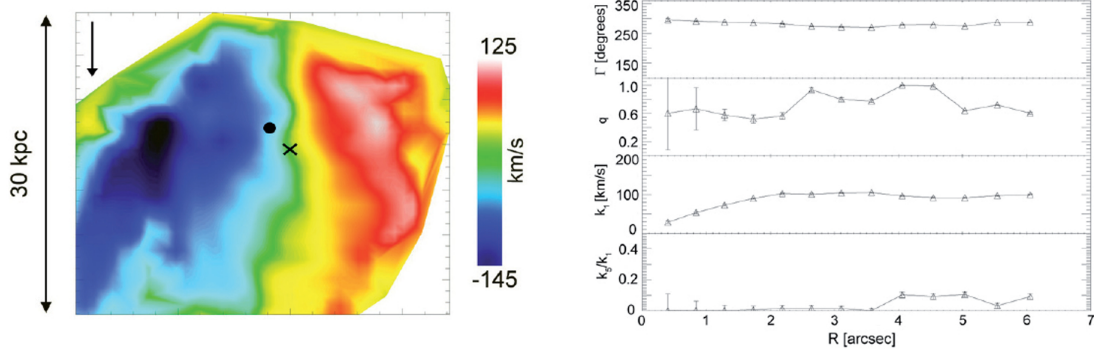


Figure 6: Velocity field of a simulated ram-pressure stripped galaxy with spatial resolution corresponding to observations at $z=0.1$ and radial profiles of some parameters determined by kinemetry (kinematic position angle, flattening, first Fourier coefficient indicating the bulk motion and normalised fifth Fourier coefficient indicating separate kinematic components). The case shown refers to edge-on ram-pressure acting already for 400Myr with black arrow indicating ICM wind direction and cross and circle the centre of kinematic and stellar disc, respectively (from Kronberger et al. 2008).

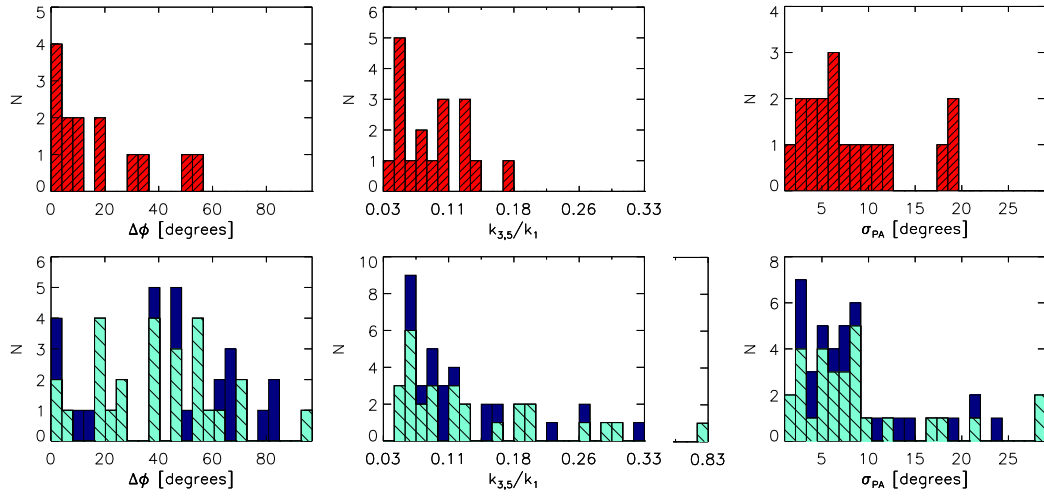


Figure 7: Abundance of galaxies distributed according to our three irregularity parameters. Top panels: local sample, bottom panels: distant field (green hashed) and cluster galaxies (blue filled histograms). Galaxies are classified irregular if $\Delta\phi > 25$, $k_{3,5}/k_1 > 0.15$ or $\sigma_{PA} > 20$ (from Kutdemir et al. 2009).